Design, Construction and Testing of a Voltage-based Maximum Power Point Tracker (VMPPT) for Small Satellite Power Supply

Masoum, Mohammad A. S.
Department of Electrical Engineering
Iran University of Science & Technology
Narmak, Tehran, 16645, Iran.

Dehbonei, Hooman
Advance Electronic Research Center
P. O. Box: 19585 - 836
Tehran, Iran.
E-mail: Dehbonei@mavara.com

***Keywords*:** Satellite, Power System, Maximum, Tracker.

Abstract

It is shown that at maximum power, the Photovoltaic (PV) voltage varies nonlinearily with temperature and isolation level, but is directly proportional to the PV cell open circuit voltage. The proportionality voltage-factor is fixed for a given PV generator regardless of temperature, isolation and panel configuration, but depends on cell material and manufacturing. This remarkable property is used to achieve temperature and insolation independent maximum power point tracking of satellite's solar cells with a simple and reliable technique. The open circuit voltage is continuously measured by a microcontroller and is used to estimate the maximum power operating point of the system.

The Voltage-based Maximum Power Point Tracker (VMPPT) is demonstrated by construction and testing of a solar battery charger (using silicon solar cells, Ni-Cd batteries and a buck mode VMPPT), a solar water pump (using silicon solar cells, a PM DC Motor and a boost mode VMPPT) and resistive loads supplied by solar cells. Measured results are satisfactory and confirm the proposed technique. The advantage of this method as compared to the current-based MPPT are "simplicity" and "higher efficiency".

1. Introduction

The satellite Electric Power Subsystem (EPS) has the responsibility of providing continuous, regulated and conditioned power to payloads and other subsystems during all mission phases. Undesired space and mission features such as eclipse and shadowing interruptions, temperature and solar angle variations, and load fluctuations as well as solar array degradation (over time) must be considered by EPS designers. In today's small spacecraft, these problems are exacerbated due to extreme mass, volume and cost constrains. Accurate sun- tracking solar arrays, generous cooling devices and high capacity batteries are denied the designer and therefore, new generation EPS are usually running with a negative power budget and every drop of available electric energy is captured and used as effectively as possible. These constrains along with the required high reliability performance and the fact that spacecraft is not mostly within the communication range, have made EPS designing exciting and challenging.

There are two general approaches for satellite power system design [1-5]. In Direct Energy Transfer (DET) method, the payload, subsystems and batteries are directly connected to the solar arrays and the extra power (at low temperatures and/or Beginning Of Life (BOL)) are absorbed by shunt regulators (Fig.1(a)). This is a dissipative and simple, but weighty and low efficient power system. A more

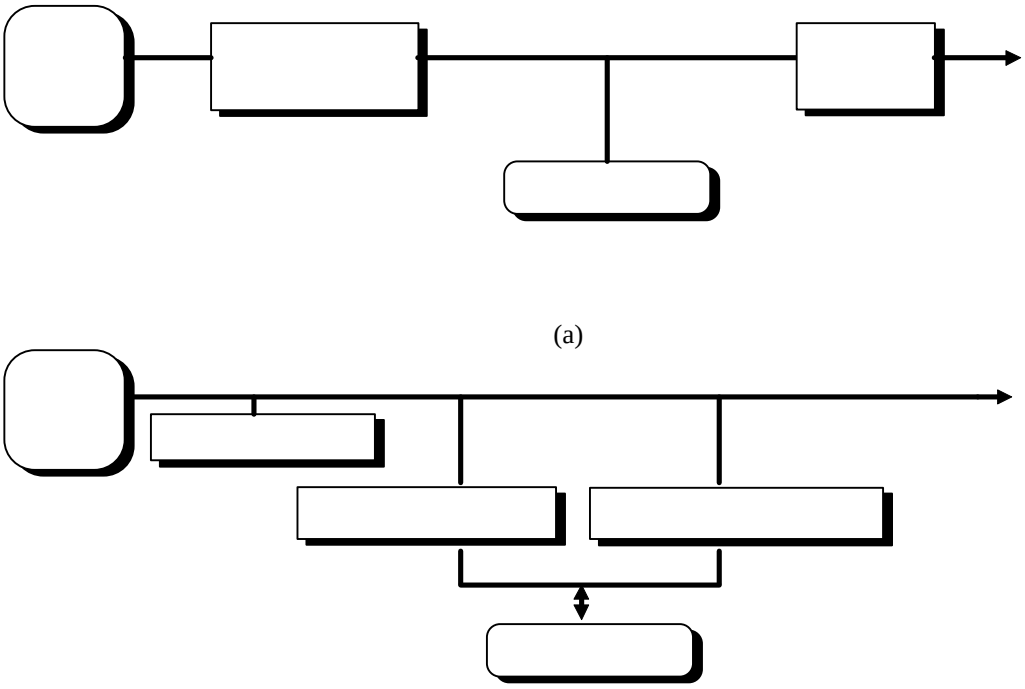

(a)

(b)

Figure 1. Block diagram of satellite Electric Power Subsystem (EPS); (a) Power Point Tracking (PPT) method., (b) Direct Energy Transfer (DET) method

common technique for designing the EPS, especially for small satellites, is the Power Point Tracking (PPT) method (Fig.1(b)): the amount of generated solar energy is continuously controlled and matched with the satellite's energy demand. The system is naturally running at a low temperature level and there will be no need for large dissipative devices. But the price is paid by the addition of a PPT device.

The primary source of power on most present satellites result from photovoltaic solar cells mounted on surfaces and illuminated by the sun's rays. In order to increase the available electrical energy and limit the required solar arrays, the ″maximum power point″ of PV cells must be actively tracked and used by the EPS system. In the literature, there are different proposed methods for Maximum Power Point Tracking (MPPT) of solar cells [6-14] and some have been applied in actual satellite power systems [15]. The current-based MPPT of [9] uses reference (dummy) cells for the measurement and estimation of ″maximum power point″ of the solar panel. In this paper, a Voltage-based MPPT is proposed for the optimal tracking of satellite solar cells. The main advantage of this method (which uses a microcontroller circuit for the online measurement of "cell open circuit voltage") as compare to the current-based MPPT method is: the elimination of the reference cells which results in a "simpler" and "more efficient" system. The effect of VMPPT is especially noticed at high power demand phases and during the EOL where the cell degradation is appreciable.

The proposed method is demonstrated by construction and testing of three laboratory PV systems: a solar battery charger (consisting of four Ni-Cd batteries with a buck type VMPPT circuit), a solar water pump (consisting of a permanent- magnet DC motor water pump and a boost type VMPPT circuit) and resistive loads supplied by solar cells .

2. Nonlinear PV Generator Characteristics

Using the equivalent circuit of photovoltaic cells (Fig.2), the expression for the nonlinear V-I characteristics of M parallel strings (N series cells per string) is

$$u_{PV} = \frac{N}{l} In\left(\frac{I_{sc} - i_{pv} + M\ I_0}{M\ I_0}\right) - \frac{N}{M} R_s\ i_{pv} \qquad (1)$$

where Io is the reverse saturation current, I_{sc} is the cell short circuit current, R_s is the series cell resistance and l is a constant coefficient proportional to cell material.

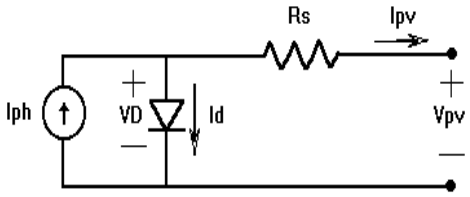

Figure 2. Photovoltaic cell equivalent circuit.

For the silicon solar panel (M=1, N=36) manufactured by the Iranian optical Fiber Fabrication Co. (OFFC), the V-I characteristics of Eq.1 can be written as

$$u_{pv} = 1.767\ \ln\left(\frac{I_{sc} - i_{pv} + .00005}{.00005}\right) - i_{pv} \qquad (2)$$

Cell specification are given in Table 1 and the computed V-I characteristics (based on equation 2) are plotted in Fig.3 for different insolation levels. The laboratory measurement of V-I and P-I characteristics for one OFFC panel are shown in Fig. 4. Comparison of these two figures indicates a good agreement between the computed and measured characteristics.

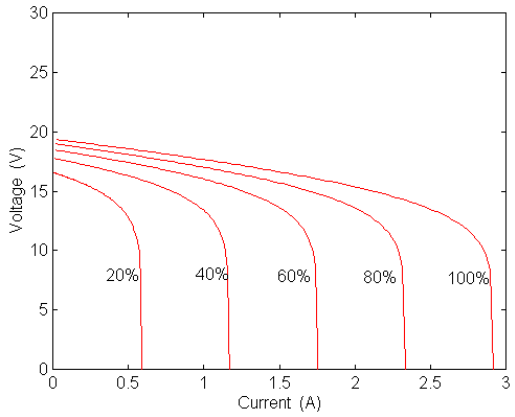

Figure 3. Computed nonlinear V-I characteristics of one OFFC silicon solar panel for different isolation levels (Eq.2)

There is also a nonlinear relationship between the V-I characteristics and operating temperature [13,14,16]. According to reference [16], this dependency can be modeled as:

$$\Delta T = T_{cell} - T_{ref}$$

$$\Delta I = a\,.\Delta T$$

$$\Delta u = -b\,.\Delta T - R_s\,.\Delta I$$

$$u_{pv}^{new-temp} = u_{pv} - \Delta u$$

$$i_{pv}^{new-temp} = i_{pv} - \Delta I \qquad (3)$$

Taking into account the impact of temperature variations (Eq.3), the new forms of Eq.2 can be written as :

$$u_{pv} = 1.69 \ln\left(\frac{3.005 - i_{pv} + .00024}{.00024}\right) - i_{pv} \quad (4a)$$

$$u_{pv} = 1.82 \ln\left(\frac{2.83 - i_{pv} + .00001}{.00001}\right) - i_{pv} \qquad (4b)$$

Equations (4a) and (4b) are evaluated for T=70°c and T=-20°c, respectively, and are plotted in Fig.5 for one OFFC panel.

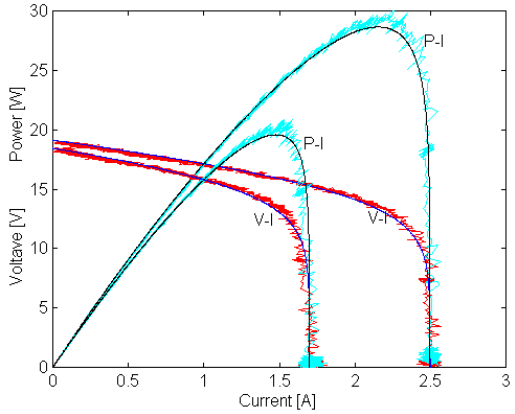

Figure 4. Measured and computed (Eq.2) nonlinear V-I and P-I characteristics of one OFFC silicon solar panel (table 1)

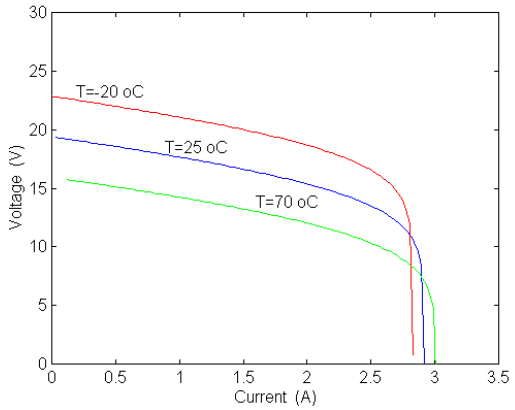

Figure 5. Temperature impact (Eqs.3,4) on V-I characteristics of OFFC silicon solar cells (table 1)

3. The Voltage-based Maximum Power Point Tracking (VMPPT)

In order to determine the operating points corresponding to maximum power for different isolation levels, the partial derivative of power is computed as follows

$$\frac{d}{di_{pv}}P = \frac{d}{di_{pv}}\left[\left(1.767\ln\left(\frac{I_{sc}-i_{pv}+.00005}{.00005}\right)-i_{pv}\right)i_{pv}\right]=0$$

(5)

The solution of Eq.5 represents the currents corresponding to maximum power as a function of short circuit currents of PV generator, $I_{mp}=f(I_{sc})$. This is the main idea for the current-based MPPT technique [9]. For the OFFC silicon cells, this function is computed as

$$\left(\frac{-35340I_{mp}}{20\times10^{3}(I_{sc}-I_{mp})+1}\right)+ \qquad (6)$$
$$1.767\ln\left(20\times10^{3}(I_{sc}-I_{mp})+1\right)-2\cdot I_{mp}=0$$

Evaluating Eq.1 at maximum power (e.g., $I_{sc}=\mathrm{I}_{\mathrm{mp}}$) and open circuit condition (e.g., $i_{pv}=0$) gives: $V_{mp}=f_1(I_{sc})$ and $V_{oc}=f_2(I_{sc})$, respectively. Therefore, at a given temperature and isolation level, the "voltage corresponding to maximum power" could be expressed as a function of "cell open circuit voltage"; namely

$$V_{mp}=g(V_{oc}) \qquad (7)$$

This is the base for the VMPPT technique. Applying numerical methods (e.g., MATHCAD Software), Eq.7 is shown by + signs in Fig.6 for the OFFC silicon solar cells.

Using curve fitting techniques, we can numerically find this relationship as:

$$V_{mp}=f_{nonlinear}(V_{oc})\cong f_{liner}(V_{oc})=$$
$$0.7\ \ V_{oc}-0.328\cong 0.7\ \ V_{OC}=m_v\ \ V_{oc} \qquad (8)$$

this equation is compared with the actual characteristics in Fig.6.

Therefore, the voltages corresponding to maximum powers are directly proportional to open circuit voltages at different isolation levels and temperatures. The proportionality voltage-factor (m_v) is fixed for a given panel regardless of cell configuration, isolation and temperature variations, but depends on cell materials and manufacturing techniques. According to Eq.8 and Fig.6, for the OFFC silicon cells $m_v=0.7$, which will also be confirmed by experimental result in the following section.

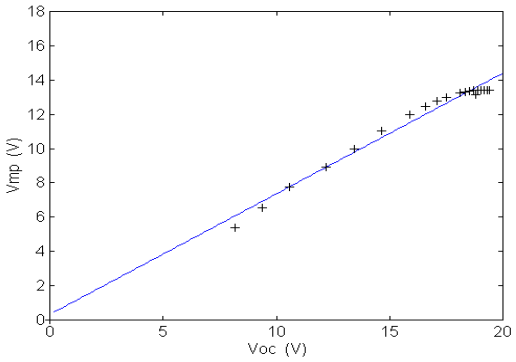

+ $Vmp = g(Voc)$

- $Vmp = 0.704 \cdot Voc + 0.328$

Figure 6. Voltages corresponding to maximum power versus open circuit cell voltages (Eq.7) and the linear function (Eq.8) approximation (T=25 and varying isolation level).

4. Construction and measurements

For the tracking and estimation of the maximum power point of solar panels, the open circuit voltage must be accurately measured under all operating conditions (temperature, isolation and degradation levels). To do this, a microsystem is used with the following responsibilities:

1. Continuous control and switching of the DC/DC converter (buck or boost mode).
2. Continuous measurement of the panel open circuit voltage.
3. Continuous estimation of panel maximum power operating point (Eq.8).
4. Continuous matching of satellite operating point with the estimated solar panel maximum power point (by changing the duty cycle of DC/DC converter).
5. If required, continuous matching of generation and demand levels by adjusting the system operating point on the V-I characteristics.

The microsystem driver circuitry consists of: a 80C51 microcontroller, D/A and A/D converters, the series-switch driver (boost), power supplies, display and keyboard as shown in Fig.7.

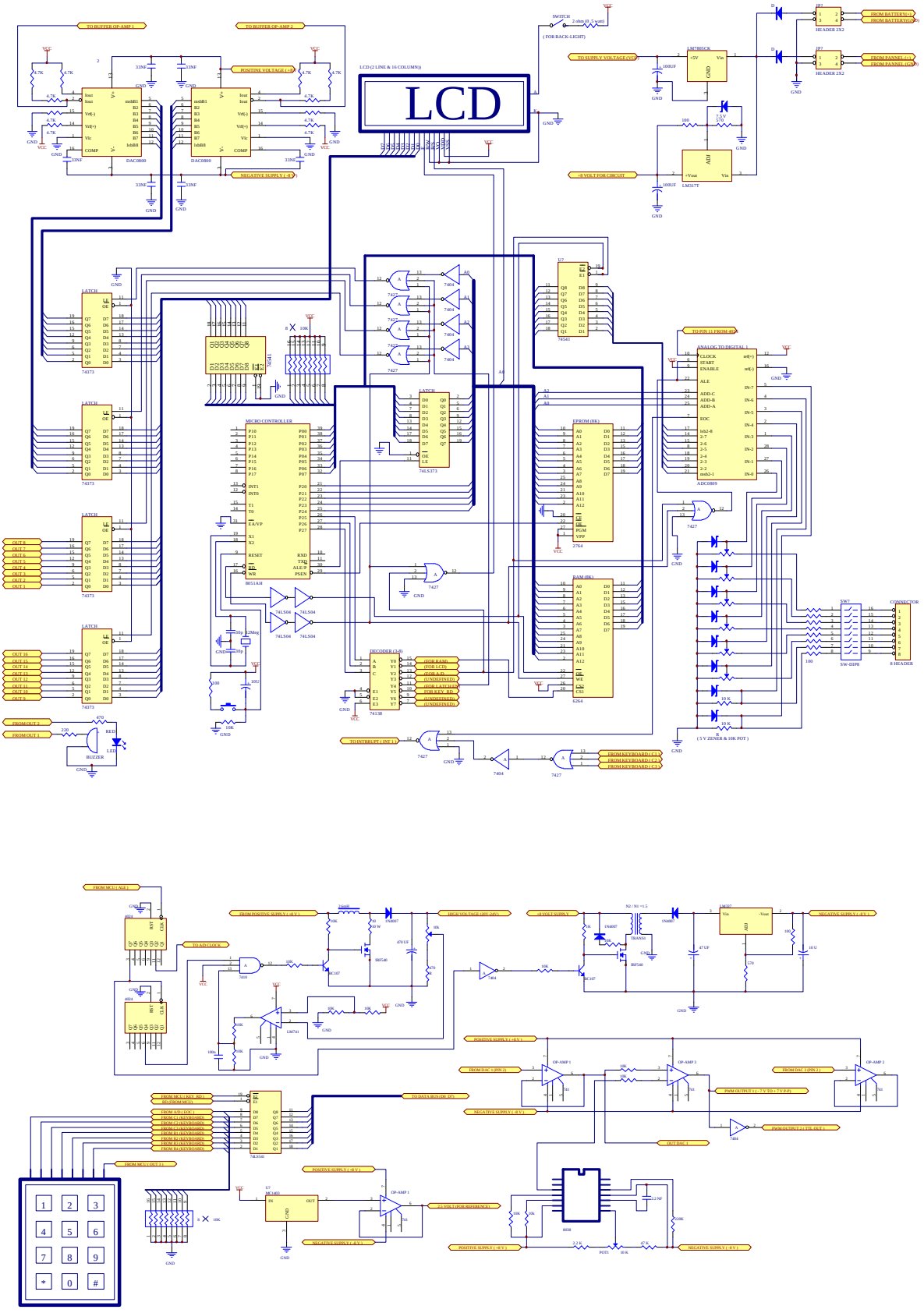

Figure 7. The microsystem driver circuitry used in Figs.8 and 12 for measurements.

4.1. A Solar Battery Charger (VMMPT in Buck Mode)

In order to experimentally investigate the performance of the proposed VMPPT tracker, the solar battery charger of Fig.8 was constructed using one OFFC silicon solar module (table 1), four Ni-Cd batteries (1.2V, 800mAh), a VMMPT buck type tracker (MOSFET power switches, ferrite core inductance) and a microcontroller (Fig.7). The measured voltage, current and power waveforms at the output of the solar panel as well as the input of the nickel-cadmium batteries are shown in figure 9, with and without the VMPPT unit. These results indicate an increase of about 150% in panel output power in the presence of VMPPT unit during the charging phases. The corresponding measured V-I and P-I characteristic for the operating condition (insolation and temperature levels) are shown in Fig.11 which confirms a maximum power of 25 watts. The two zero-power instances on panel waveform, indicate disconnection of panel by the microsystem and online measurement of its open circuit voltage

Experiments and measurements at different isolation, temperature and load levels using various voltage-factors (Fig.11), confirmed that maximum output power is obtained for a unique value of

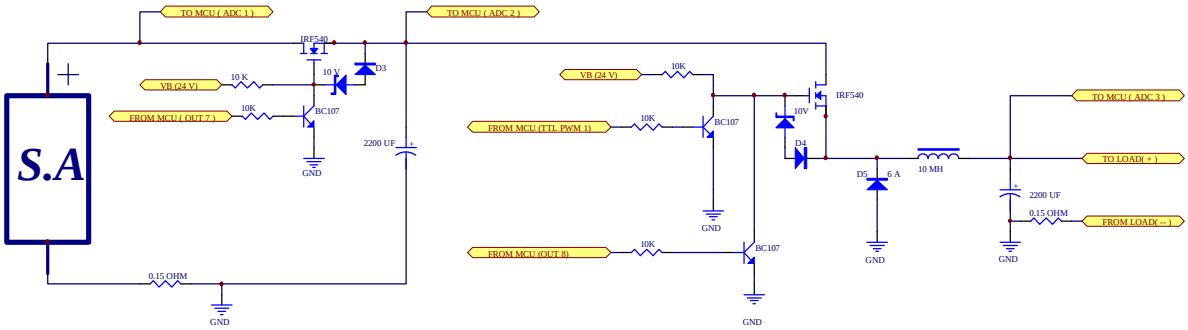

Figure 8. The constructed microcontroller-based solar battery charger (VMPPT in buck mode) used for measurements

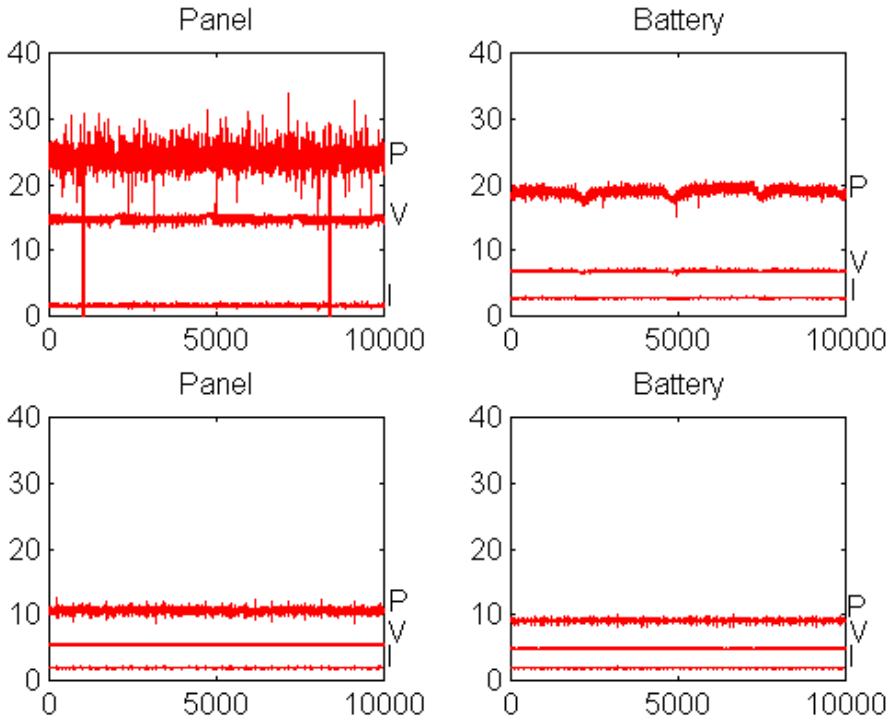

Fig 9. The waveforms of current, voltage and power at the output of the solar panel and the input of the batteries with (top figures) and without (bottom figures) the VMPPT unit. Horizontal axis indicates sampling times.

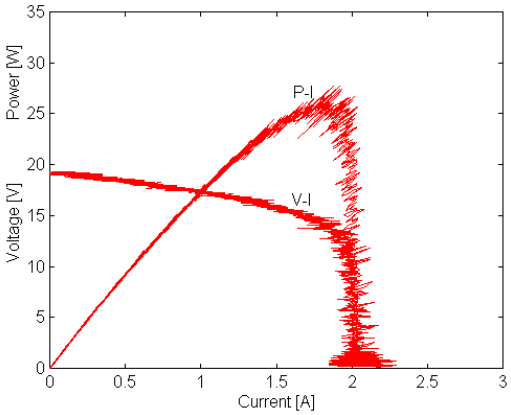

Figure 10. The measured V-I and P-I characteristics corresponding to Fig.9.

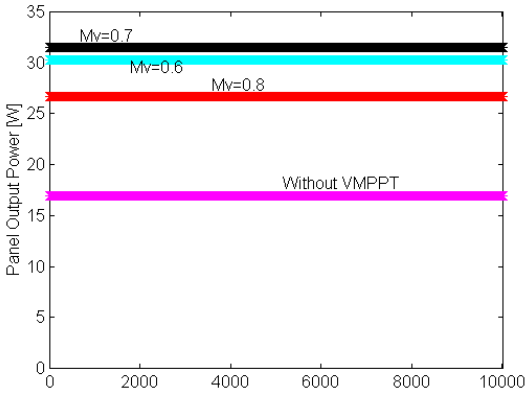

Figure 11. Comparison of measured panel output power (of solar battery charger) for different values of voltage-factors. The operating conditions (insolation level) of Fig.10 & 11 are different.

$m_v = 0.7$.

4.2. A Solar Water Pump (VMPPT in Boost Mode)

The solar water pump of Fig.12 was constructed using one OFFC silicon solar module (Table 1), a small permanent magnet DC motor (24 V, 45W), a VMPPT boost type tracker and a microcontroller (Fig.7). Different measured results for various values of voltage-factor (Fig.13) confirm the unique value of $m_v = 0.7$ for maximum power operation of the system under different conditions.

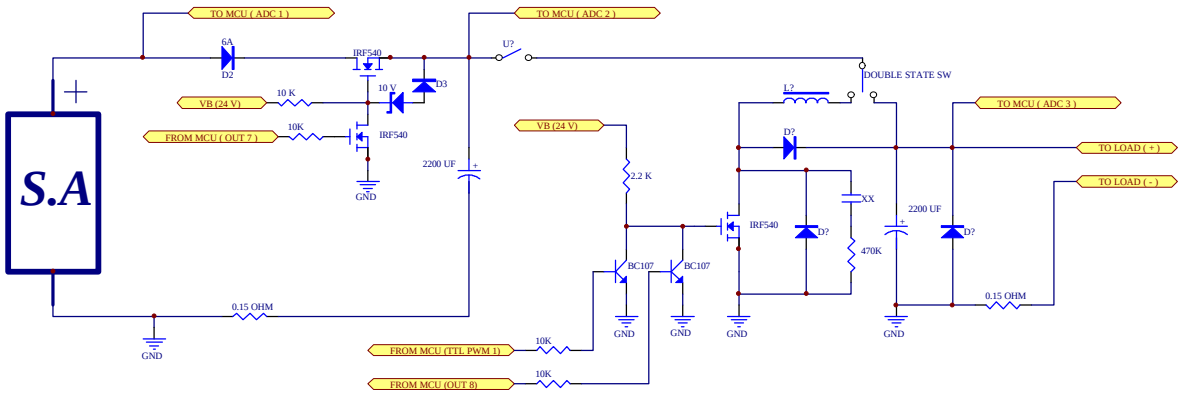

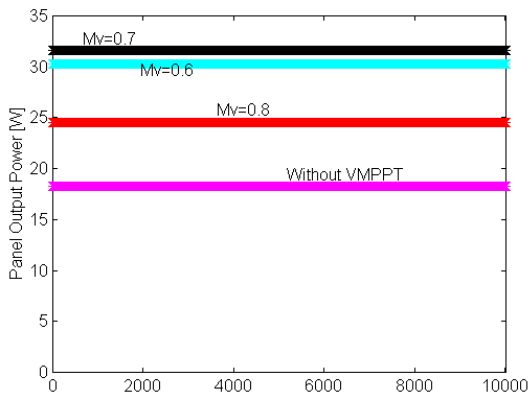

Figure 13. Comparison of measured panel output power (of solar water pump) for different values of voltage-factors. The operating conditions (insolation level) of Fig.13 and 14 are different.

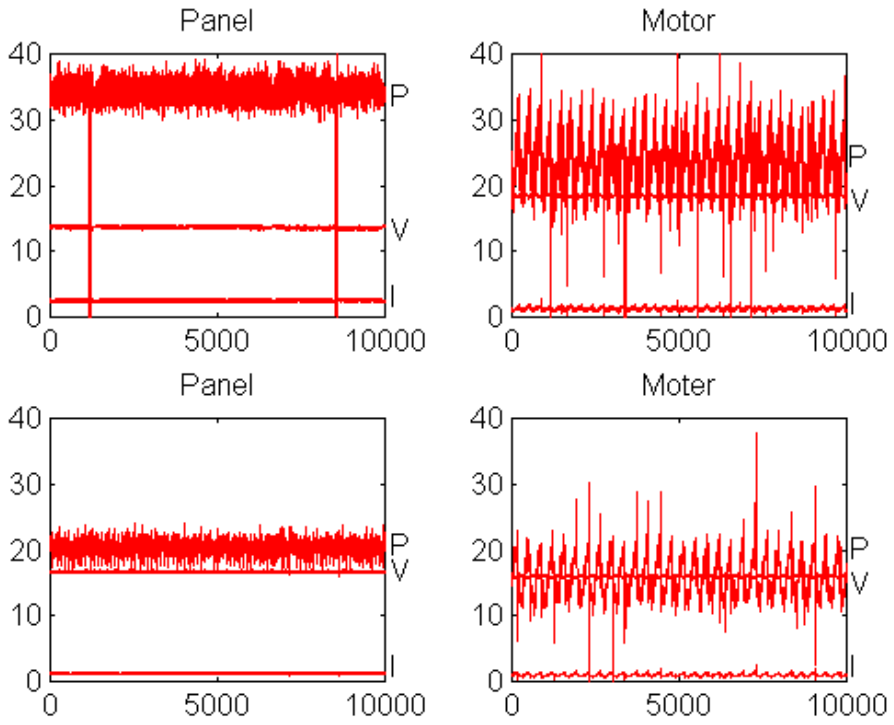

Fig 15. The waveforms of current, voltage and power at the output of the solar panel and the input of solar pump with (top figures) and without (bottom figures) the VMPPT unit.

Figures 14 and 15 demonstrate the V-I and P-I characteristics as well as voltage, current, and power waveforms for a chosen operating condition. The introduction of VMPPT changes the panel output power from 22 watts to 34 watts (55% increase).

4.3. Resistive Loads Supplied by Solar Cells (VMPPT in Buck Mode)

Further experimental investigations of VMPPT technique was done by supplying a set of resistors with one OFFC silicon solar panel (Table 1). Different measurements were performed to investigate the uniqueness of voltage-factor for different isolation, temperature and load conditions. As an example, figure 16 shows the measured panel average output power with and without the VMPPT tracker for a chosen operating condition. As for the other types of loads (Figs.11 and 13), the computed value of voltage-factor $(m_v = 0.7)$ results in maximum output power.

Figures 17-19 show the V-I and P-I characteristics and the corresponding waveforms for two resistive loads. According to Fig.17, the maximum output solar power (for the chosen operating condition) is 32W. Furthermore, the panel voltage corresponding to maximum power $(Vmp = 18V)$ is about 70% of

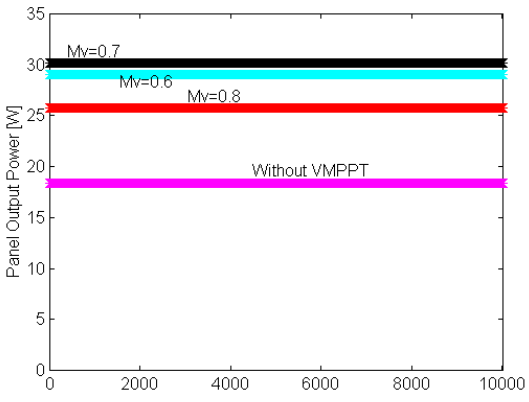

Figure 16. Comparison of measured panel output (of resistive loads) for different values of voltage-factor.

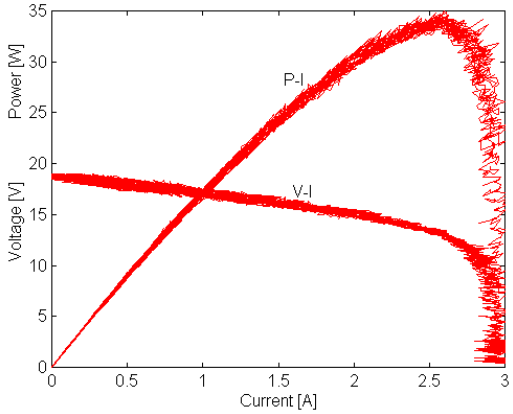

Figure 14. The measured V-I and P-I characteristic corresponding to Fig.15.

the panel open circuit voltage $(V_{oc} = 12.6V)$ which confirms the unique computed value of the voltage-factor $(m_v = 0.7)$ for these loads.

The impact of VMPPT is 125% and 28% increase in panel output power for the heavy (Fig.18) and light (Fig.19) resistive loads , respectively.

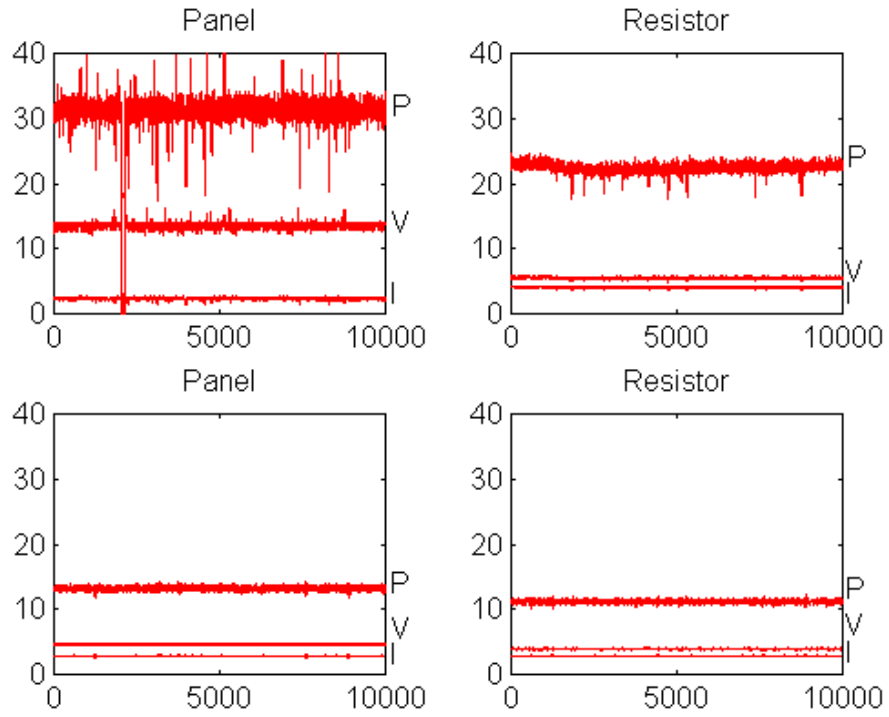

Fig 18. The waveforms of current, voltage and power at the output of the solar panel and the input of the resistive load with (top figures) and without (bottom figures) the VMPPT unit (heavy loads).

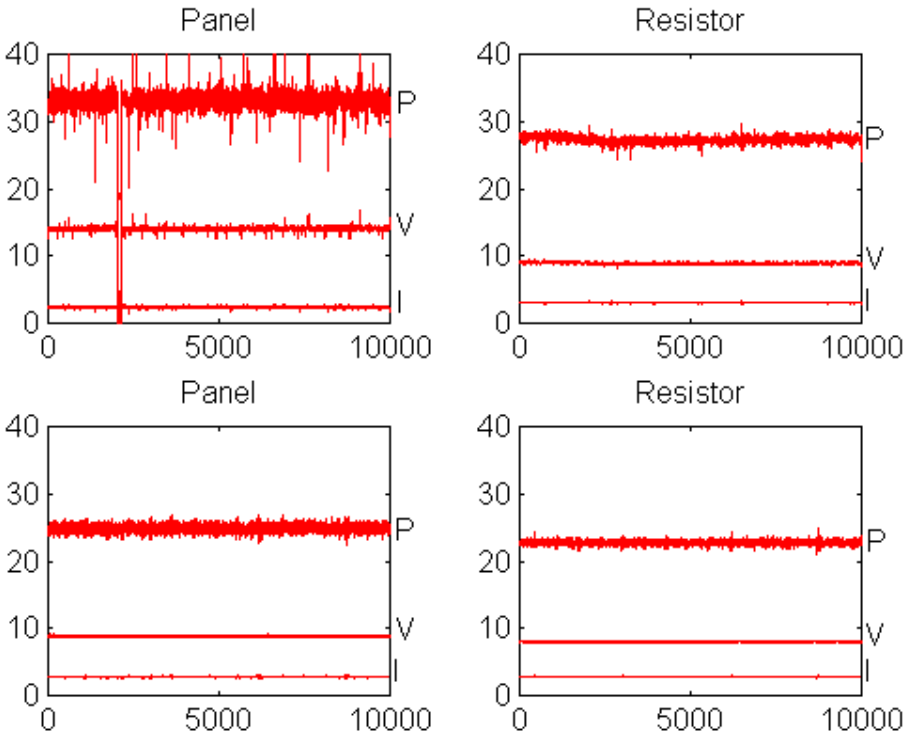

Fig 19. The waveforms of current, voltage and power at the output of the solar panel and the input of the resistive load with (top figures) and without (bottom figures) the VMPPT unit (light loads).

Figure 17. The measured V-I and P-I characteristics corresponding to Figs.18 and 19.

5. Conclusion

A Voltage-base Maximum Power Point Tracker (VMPPT) is proposed for optimal Power Point Tracking (PPT) of Satellite Electric Power Subsystem (EPS) and is demonstrated by construction and testing of a solar battery charger, a solar water pump and resistive loads. It is shown (numerically and experimentally) that at maximum power, the cell voltage is linearly proportional to the cell open circuit voltage.

A microsystem is used for the on-line measurement of the solar cells open circuit voltage, estimation of panel maximum power point, control of system operating point and matching it with panel maximum power point on the V-I characteristic curves. The proportionality factor is fixed (e.g., $m_V = 0.7$ for OFFC silicon cells) regardless of operating conditions. The following conclusions can be stated:

1. Introduction of VMPPT increases the output power of PV generators. The percentage of power increase depends on operating conditions (isolation, temperature, degradation and load levels).

2. The proposed VMPPT technique is very simple since it requires only the measured open circuit voltage.

3. The cell open circuit voltage can be measured using a microsystem.

4. The same microsystem can be used for switching of DC/DC converters (buck or boost mode) and controlling the operating point on the panel V-I characteristics.

5. The effect of VMPPT is especially appreciable when generated electrical energy is less than the demand level (e.g., at EOL, high power demand phases, high temperature conditions).

6. The main advantage of the proposed microprocessor-based VMPPT method as compared to the current-based MPPT [9] is the elimination of the reference cells which results in a “simpler” and “more efficient” system.

6. References

[1] Chetty, P.R.K., “Satellite Technology and its Applications”, TAB BOOKS Inc., 1988.

[2] Sullivan, R.M., “The Small Astronomy Satellite (SAS) Power system”, 4th Annual AIAA/USU Conference on Small Satellite, 1990.

[3] Wong, H.S., Blewett, M.J. “The UoSAT-2 Spacecraft Power system”, Journal of the Institution of Electronic and Radio Engineering, Vol. 57, No.5, Sep./Oct. 1987.

[4] Sakoda, D., Nobel, M., Paluszek, S. “Preliminary design of PANSAT Electric power and Communication Subsystems”, 4th Annual AIAA/USU Conference on Small Satellite, 1990.

[5] Dunbar, R., Hardman, G. “A Flexible Autonomous Power Management System for Small Spacecraft”, 4th Annual AIAA/USU Conference on Small Satellite, 1990.

[6] Enslin, J.H.R., Snyman, D.B., ”Combined Low-Cost, High-Efficient Inverter, Peak Power Tracker and Regulator for PV Application”, IEEE, T-PE, VOL.6, NO.1, January 1991.

[7] Saied, M.M., Hanafy, A.A., EL_Gabaly, M.A., Safa, Y.A., Jaboori, M.G., Yamin, KH.A., Sharaf, A.M., ”Optimal Design Parameter for a PV Array Coupled to a DC Motor via a DC-DC Transformer”, IEEE, 91WM 146-1EC.

[8] Jaboori, M.G., Saied, M.M., Hanafy, A.A.R., ”A Contribution to the Simulation and Design Optimization of Photovoltaic Systems”, IEEE, 91WM 149-5EC.

[9] Alghuwainem, S.M., ”Matching of DC Motor to a Photovoltaic Generator Using a STEP-UP Converter with a Current-Locked Loop”, IEEE, T-EC, VOL.9, NO.1, March 1994.

[10] Hiyama, T., Kouzoma, Sh., Imakubo, T., ”Identification of Optimal Operating Point of PV Modules Using Neural Network for Real Time Maximum Power Tracking Control”, IEEE, T-EC, VOL.10, NO.2, June 1995.

[11] Hiyama, T., Kouzoma, Sh., Imakubo, T., ”Evaluation of Neural Network Based Real Time Maximum Power Tracking Controller for PV System”, IEEE, T-EC, VOL.10, NO.3 September 1995.

[12] Altas, I.H., Sharaf, A.M., ”A Novel On-line MPP Search Algorithm for PV Arrays”, IEEE, T-EC, VOL.11, NO.4, December 1996.

[13] Dehbonei, H., "Solar Water Pump, Using a Maximum Power Point Tracker (MPPT) for Optimal Driving a DC Motor Pump": IUST, Electrical Engineering Department, M.S Thesis, September 1997, (Persian).

[14] Masoum, M.A.S., Dehbonei, H., “Optimal Power Point Tracking of Photovoltaic Systems under all Operating Conditions”, I7th Congress of the World Energy Council, Houston, USA, Sep 12-18, 1998.

[15] Beukes, H.J., Enslin, J.H.R., ”Analysis of a New Compound Converter and Bus Regulator for Satellite Power Systems”, IEEE, PESC, 1993.

[16] Salameh, Z.M., Borowy, B.S., Amin, A.R.A., ”Photovoltaic Modules-Site Matching Based on the Capacity Factors”, IEEE, T-EC, VOL.10, NO.2, June 1995.